Translational Oncology
www.transonc.com

Volume 11 Number 6 December 2018 pp. 1390–1397 1390

Clinical Relevance of Genomic Changes in Recurrent Pediatric Solid Tumors

Boram Lee[*,†,1], Ji Won Lee[‡,1], Joon Ho Shim[*,†,1], Je-Gun Joung[*], Jae Won Yun[*], Joon Seol Bae[*], Hyun-Tae Shin[*], Ki Woong Sung[‡] and Woong-Yang Park[*,†,§]

[*]Samsung Genome Institute, Samsung Medical Center, 81 Irwon-ro, Gangnam-gu, Seoul 06351, Republic of Korea; [†]Department of Health Science and Technology, Samsung Advanced Institute for Health Sciences and Technology, Sungkyunkwan University, 81 Irwon-ro, Gangnam-gu, Seoul 06351, Republic of Korea; [‡]Department of Pediatrics, Samsung Medical Center, Sungkyunkwan University School of Medicine, 81 Irwon-ro, Gangnam-gu, Seoul 06351, Republic of Korea; [§]Department of Molecular Cell Biology, Sungkyunkwan University School of Medicine, 81 Irwon-ro, Gangnam-gu, Seoul 06351, Republic of Korea

Abstract

PURPOSE: Relapsed/refractory pediatric cancers show poor prognosis; however, their genomic patterns remain unknown. To investigate the genetic mechanisms of tumor relapse and therapy resistance, we characterized genomic alterations in diagnostic and relapsed lesions in patients with relapsed/refractory pediatric solid tumors using targeted deep sequencing. *PATIENTS AND METHODS:* A targeted sequencing panel covering the exons of 381 cancer genes was used to characterize 19 paired diagnostic and relapsed samples from patients with relapsed/refractory pediatric solid tumors. *RESULTS:* The mean coverage for all samples was 930.6× (SD = 213.8). Among the 381 genes, 173 single nucleotide variations (SNVs)/insertion-deletions (InDels), 100 copy number alterations, and 1 structural variation were detected. A total of 72.6% of SNVs in primary tumors were also found in recurrent lesions, and 27.2% of SNVs in recurrent tumors had newly occurred. Among SNVs/InDels detected only in recurrent lesions, 71% had a low variant allele fraction (<10%). Patients were classified into three categories based on the mutation patterns after cancer treatment. A significant association between the major mutation patterns and clinical outcome was observed. Patients whose relapsed tumor had fewer mutations than the diagnostic sample tended to be older, had longer progression-free survival, and achieved complete remission after relapse. Contrastingly, patients whose genetic profile only had concordant mutations without any change had the worst outcome. *CONCLUSIONS:* We characterized genomic changes in recurrent pediatric solid tumors. These findings could help to understand the biology of relapsed childhood cancer and to develop personalized treatment based on their genetic profile.

Translational Oncology (2018) 11, 1390–1397

Introduction

The outcome of pediatric cancer has greatly improved over the past few decades, resulting in a 5-year overall survival of around 80% [1]. However, certain high-risk or relapsed/refractory pediatric cancers still show poor prognosis, with a survival rate of less than 20%. These findings suggest the urgent need for new therapeutic strategies. Advances in genomic technologies in recent years have improved our ability to detect diverse somatic and germline genomic aberrations in cancer. It is

Address all correspondence to: Je-Gun Joung or Woong-Yang Park, Samsung Genome Institute, Samsung Medical Center, 81 Irwon-ro, Gangnam-gu, Seoul 06351, Republic of Korea. E-mail: jegun.joung@samsung.com

[1] These authors contributed equally to this work.

Received 16 July 2018; Revised 27 August 2018; Accepted 27 August 2018

1936-5233/18
https://doi.org/10.1016/j.tranon.2018.08.013

anticipated that the interpretation of genomic information from cancer could be used to develop new therapeutics. In particular, as the mutation number is relatively small in childhood cancer, unlike adult cancers, which are caused by the accumulation of mutations from environmental influences [2], it has been proposed that pediatric cancer could be a good candidate to find therapeutic targets using genomic analysis [3].

Previous studies have reported the genetic heterogeneity at relapse in diverse cancer types [4–6]. These studies suggested that new additional key mutations and clonal evolution might contribute to tumor relapse. During tumor evolution, subclonal mutations acquired under the selective pressure of previous therapy might confer resistance [7]. Intrinsic tumor heterogeneity might also cause genetic heterogeneity at tumor relapse. Most studies on relapsed tumors have focused on adult cancer patients, while there have been few studies comparing genetic variations of both samples at diagnosis and recurrence in childhood cancer.

Recently, a cancer panel using high-depth next-generation technology has attracted attention as a tool to identify mutations in a large number of oncogenes [8,9]. The panel can provide sensitive detection of cancer-specific mutations and can identify rare mutations and minor alleles with lower variant allele fractions (VAFs) [10]. Sensitive detection of actionable variants, especially in tumor tissues from refractory cancer, is an essential step toward personalized cancer medicine.

To investigate the genetic mechanisms linked to tumor relapse and therapy resistance, we detected and characterized genomic alterations between primary lesions and its relapsed lesion in patients with pediatric solid tumors using high-depth targeted panel sequencing.

Materials and Methods

Patients and Sample Preparation

Patients with relapsed/refractory pediatric solid tumors who had samples taken at both diagnosis and relapse were included in this study. This study was approved by the Institutional Review Board of Samsung Medical Center (IRB approval no. SMC 2015-11-053), and written informed consent was obtained from the participants and/or their parents or legal guardians.

Isolation of Genomic DNA

Both fresh-frozen (FF) tissue and formalin-fixed, paraffin-embedded (FFPE) tissue were used. All tumor specimens were reviewed by a pathologist to determine the percentage of viable tumor and their adequacy for sequencing. Genomic DNA from FFPE tissue was extracted using a Qiagen DNA FFPE Tissue kit, and genomic DNA from FF tissue was extracted using a QIAamp DNA mini kit (Qiagen, Valencia, CA). The genomic DNA concentration and purity were measured using a Nanodrop 8000 UV–Vis spectrometer (Thermo Scientific Inc., Wilmington, DE) and a Qubit 2.0 Fluorometer (Life technologies Inc., Grand Island, NY). To estimate DNA degradation, DNA median size and ΔCt (cycle threshold) values were measured using a 2200 TapeStation Instrument and real-time PCR (both Agilent Technologies, Santa Clara, CA), respectively.

Sequencing Using a Cancer Panel (CancerSCAN)

Genomic DNA (250 ng) from each tissue was sheared in a Covaris S220 ultrasonicator (Covaris, Woburn, MA) and used to construct a library using CancerSCAN [10,11] probes and a SureSelect XT reagent kit (HSQ; Agilent Technologies) according to the manufacturer's protocol. This panel is designed to enrich exons of 381 genes curated from the literature (Supplementary Table S1). After the enriched exome libraries were multiplexed, the libraries were sequenced using the 100-bp paired-end mode of the TruSeq Rapid PE Cluster Kit and TruSeq Rapid SBS kit on the Illumina HiSeq 2500 sequencing platform (Illumina Inc., San Diego, CA). The DNA sequence data were aligned to the human genome reference (hg19) using the MEM algorithm in BWA 0.7.5 [12]. Duplicate read removal was performed using Picard v.193 and SAMTOOLS v0.1.18 (samtools.sourceforge.net). Local alignment was optimized using the Genome Analysis Toolkit (GATK) v3.1-1 (https://software.broadinstitute.org/gatk/). We also used BaseRecalibrator from GATK for base recalibration based on known single nucleotide polymorphisms (SNPs) and insertion-deletion (InDel) from Mills, dbSNP138, and 1000G gold standard, 1000G phase1, and Omni 2.5.

SNV and InDel Detection

Variant calling was done only in regions targeted in CancerSCAN [10]. We detected single nucleotide variations (SNVs) using two tools: MuTect and LoFreq [13,14]. We then filtered out falsely detected variants from abnormally aligned strand biased and clustered reads using in-house–developed scripts. ANNOVAR was used to annotate the

Table 1. Patient Characteristics of Relapsed Childhood Cancers

Patient ID	Sex	Age at Diagnosis (Years)	Diagnosis	First-Line Treatment	Interval from Diagnosis to Relapse (Months)	Outcome
1	M	17.3	Rhabdomyosarcoma	CTx, high-dose CTx	15.6	Progression
2	M	2.7	Rhabdomyosarcoma	CTx	15.4	Progression
3	M	0.3	Malignant rhabdoid tumor	Surgery, CTx, RT (brain)	6.1	Progression
4	M	15.3	Osteosarcoma	CTx, surgery	51.0	CR
5	M	9.6	Neuroblastoma	CTx, surgery	15.3	Progression
6	F	8.8	Rhabdomyosarcoma	CTx, RT, high-dose CTx including TBI	16.5	Progression
7	F	5.4	Glioblastoma	Surgery, CTx, RT, high-dose CTx	21.6	Progression
8	F	3.3	Hepatoblastoma	CTx, surgery	6.7	Progression
9	F	14.4	Rhabdomyosarcoma	CTx, RT	25.3	CR
10	M	12.8	Rhabdomyosarcoma	CTx	3.3	CR
11	M	0.8	Epithelioid sarcoma	CTx	4.2	Progression
12	F	15.4	Neuroblastoma	Surgery, CTx	16.0	CR
13	F	2.9	Wilms tumor	CTx	6.0	CR
14	M	13.8	Desmoplastic small round cell tumor	CTx	3.6	Progression
15	F	3.0	Ganglioneuroblastoma	Surgery, CTx	15.4	CR
16	M	18.5	Medulloblastoma	Surgery, CTx, RT, high-dose CTx	25.6	PR
17	M	3.8	Neuroblastoma	Surgery, CTx, RT, high-dose CTx, MIBG	16.3	Progression
18	F	3.4	Neuroblastoma	CTx, Surgery	8.5	Progression
19	F	10.5	Angiosarcoma	Surgery, CTx	10.1	PR

Abbreviations: *CTx*, chemotherapy; *RT*, radiotherapy; *TBI*, total body irradiation; *MIBG*, metaiodobenzylguanidine therapy; *CR*, complete remission; *PR*, partial remission.

Table 2. Summary of Tumor Type and Mutation

Tumor Type	Patients	Previously Reported Driver Mutation	Detected Mutation
Neuroblastoma	pt. 5, 12, 15, 17, 18	*MYCN* amplification, *ALK*, *PTPN11*, *NRAS* mutation, *ATRX* mutation or deletion [16]	*MYCN* amplification and *PTPN11* deletion in pt. 18
Rhabdomyosarcoma	pt. 1, 2, 6, 9, 10	*PAX3/FOXO1* fusion, *PAX7/FOXO1* fusion, *NRAS*, *KRAS*, *HRAS*, *FGFR4*, *PIK3CA*, *CTNNB1* mutation, *MYCN*, *MDM2*, *CDK4* amplification [17]	*MYCN* amplification in pt. 1 and 6 *MDM2* amplification in pt. 2 *RB1* mutation in pt. 10
Malignant rhabdoid tumor	pt. 3	*SMARCB1* loss [18]	*SMARCB1* exon 6 deletion in pt. 3
Epitheloid sarcoma	pt. 11	*SMARCB1* loss [19]	*SMARCB1* deletion in pt. 11
Desmoplastic small round cell tumor	pt. 14	*WESR1/WT1* fusion [20]	*WESR1/WT1* fusion in pt. 14
Osteosarcoma	pt. 4	*TP53*, *RB1*, *CDKN2A* mutation or deletion, *MDM2* amplification, *MYC* amplification [21], *PIK3CA*, *KRAS* mutation [22]	*KRAS* mutation, *TP53* and *RB1* frameshift mutation, *MYCN* amplification in pt. 4
Angiosarcoma	pt. 19	*PTPRB*, *PLCG1* mutation [23], *TP53* mutation, *CDKN2A* deletion, *MYC* amplification [24]	*TP53* mutation in pt. 19
Wilms tumor	pt. 13	*WT1*, *WTX*, *CTNNB1*, *FWT1*, *FWT2* mutation [25]	*CTNNB1* mutation in pt. 13
Hepatoblastoma	pt. 8	*CTNNB1*, *APC*, *NFE2L2* mutation, *TERT* promoter mutation [26]	-
Glioblastoma	pt. 7	*H3F3A*, *HIST1H3B*, *HIST1H3C*, *BRAF*, *ATRX*, *FGFR1*, *ACVR1*, *TP53*, *SETD2* mutation, *PDGFRA*, *MYC*, *MYCN* amplification, *CDKN2A* deletion, *NTRK* fusion [27]	*NRAS* and *TP53* mutation, *MYCN* amplification in pt. 7
Medulloblastoma	pt. 16	*CTNNB1*, *PTCH1*, *MLL2*, *SMARCA4*, *TP53*, *DDX3X* mutation [28]	*APC* mutation in pt. 16

detected variants using diverse resources, including dbSNP138, COSMIC, TCGA, and in-house Korean SNP DB. InDels were detected using Pindel [15] and annotated using ANNOVAR. To filter out germline variants, we applied two algorithms: 1) except for hotspot mutations, variants with an allele frequency greater than or equal to 97% were filtered out, and 2) suspected germline variants were filtered out if the allele frequency was greater than or equal to Korean normal samples.

Copy Number Alteration Detection

We used CancerSCAN software to detect copy number alteration (CNA) [10]. In CancerSCAN, the software 'Depth of Coverage' in GATK v3.1-1 was used to calculate the sequencing coverage for each exon. The mean coverage for the total exons was calculated and normalized by pattern matched normal reference datasets. Tumor purity to adjust the CNA was calculated using normalized coverage and B allele frequencies. We identified copy number deletion when the copy number was less than 0.7 and copy number amplification when the copy number was more than four using the above method. Low-level copy number gain and copy number loss were identified using B allele frequencies. We defined a copy number of three as low-level copy number gain and a copy number of one as low-level copy number loss. Exon 6 deletion of *SMARCB1* was detected manually by calculating normalized copy number of each exon.

Statistics

Differences between categorical variables were measured using Fisher's exact test. Differences between means in continuous variables were calculated using Wilcoxon rank sum test, and comparisons between

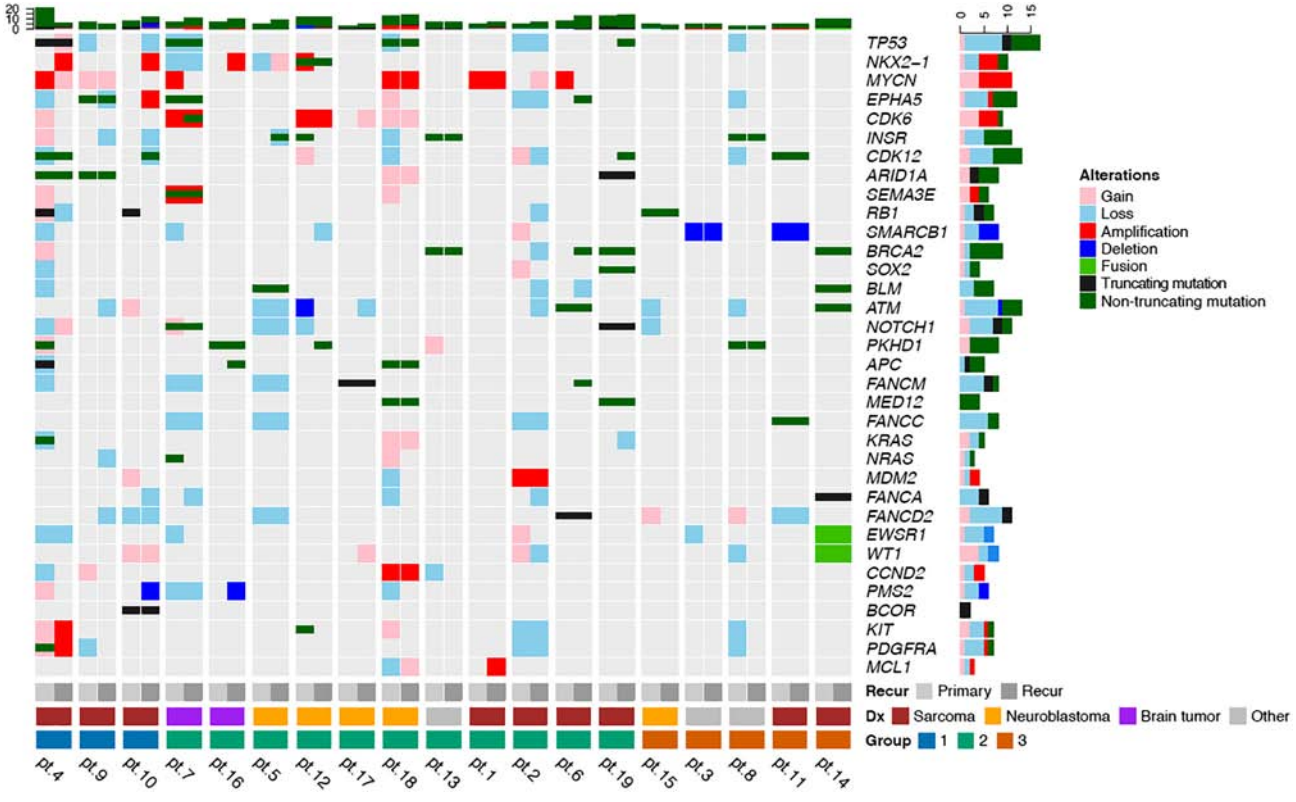

Figure 1. Landscape of genetic alterations. Diagram of the landscape of alterations of paired diagnostic-relapse samples.

continuous variables in the three groups were performed using the Kruskal-Wallis test. The Kaplan-Meier method and log-rank univariate comparisons were used to estimate survival. R version 3.4.1 was used for all statistical analyses, and $P < .05$ was accepted as statistically significant.

Results

Patient characteristics

Nineteen patients with various diagnoses, including five rhabdomyosarcomas and five neuroblastomas, were enrolled in this study. Detailed information for each patient is summarized in Table 1. All patients received chemotherapy before relapse or progression, and five of them underwent high-dose chemotherapy because of the high probability of relapse after standard treatment. Six patients received radiotherapy as a part of the first-line treatment, and the biopsy sites at relapse were irradiated in three of them (patients 6, 7, and 16). Median time to relapse/progression was 15.4 months (range, 3.3-51.0 months). Eleven patients had recurrences after completing the scheduled first-line treatment, and eight patients experienced disease progression during treatment. Eleven patients showed disease progression again after salvage treatment, six patients achieved complete remission, and two patients were in partial remission.

Detected Genetic Alterations

We carried out targeted sequencing on 19 paired samples. Based on the sequence analysis, the average target depth for all samples was 930.6× (SD = 213.8) (Supplementary Table S2). Across the 381 target genes, 173 SNVs/InDels, 100 CNAs, and 1 structural variation (*EWSR1-WT1* fusion in patient 14) were detected (Supplementary Tables S3, S4). The detected alterations are summarized in Table 2 [16–28]. The landscape of these alterations is shown in Figure 1. The most frequently altered genes were *TP53* (six SNVs/InDels) followed by *PKHD1* (n = 5), *BRCA2* (n = 4), *INSR* (n = 4), *CDK12* (n = 4), *LRP1B* (n = 3), *NOTCH1* (n = 3), *EPHA5* (n = 3), *RB1* (n = 3), *NOTCH3* (n = 3), *ARID1A* (n = 3), and *APC* (n = 3). Frequently amplified genes were *MYCN* (n = 5) and *NKX2–1* (n = 4). *MYCN* amplifications with a copy number greater than eight were present in three cases. The copy number of *MYCN* ranged from 22.2 to 156.6 in these cases. Other genes with high-level amplification were *MCL1*, *MDM2*, *PRDM1*, *CCND2*, *FGF6*, *FGF23*, *CDK6*, *SEMA3A*, *SEMA3E*, *KIT*, and *PDGFRA*. *FGF6* and *FGF23* are 62 kbp and 128 kbp apart from *CCND2* and were amplified in the same tumors showing *CCND2* amplification. Frequently deleted genes were *PMS2* (n = 2) and *SMARCB1* (n = 2). Only exon 6 out of the nine exons of *SMARCB1* was deleted in patient 3, who was diagnosed as having a malignant rhabdoid tumor. In this patient, the B allele frequencies of almost all the SNPs on chromosome 22 were near 5%, 95%, or 100%; in other words, there was loss of heterozygosity in chromosome 22 in this patient, resulting in the homozygous deletion of *SMARCB1* exon 6 (Figure 2).

Comparison of Genetic Alterations between Diagnosis and Recurrence

A total of 72.6% of SNVs in diagnostic lesions were also found in the recurrent lesions, and 27.2% of SNVs in recurrent tumors had newly occurred. The tumor mutation burden of the recurrent tumor increased in nine patients (47%), decreased in three patients (16%), and did not change in seven patients (37%).

We found several patterns in the changes of genetic variations between the diagnostic and relapsed samples (Figure 3). For example, patient 4 had high number of SNVs/InDels that were present in the diagnostic tumor but disappeared in the recurrent lesions, indicating clonal extinction of tumor cells. Patient 6 had a relatively high number of SNVs/InDels that newly occurred in the recurrent lesion, indicating additional clonal expansion of tumor cells. However, patients 3, 8, 11, 14, and 15 had no disappearing or additionally acquired SNVs/InDels in their recurrent lesions. Consequently, we classified these patterns into three groups. A patient was classified into group 1 when the number of disappearing SNVs and InDels in the recurrent lesion was more than the number of newly acquired SNVs and InDels. A subject was classified into group 2 when the number of disappearing SNVs and InDels was less than or equal to the number of newly acquired SNVs and InDels. A patient was classified into group 3 when no SNVs or InDels disappeared or were newly acquired.

One patient with osteosarcoma and two with rhabdomyosarcoma comprised group 1. Eleven patients with various tumor types were classified into group 2. The diagnoses of the five patients classified into group 3 were malignant rhabdoid tumor, hepatoblastoma, epithelioid sarcoma, ganglioneuroblastoma, and desmoplastic small round cell tumor. Patients in group 1 tended to be old, and patients in group 3 tend to be young (Table 3). All patients in group 1 achieved complete

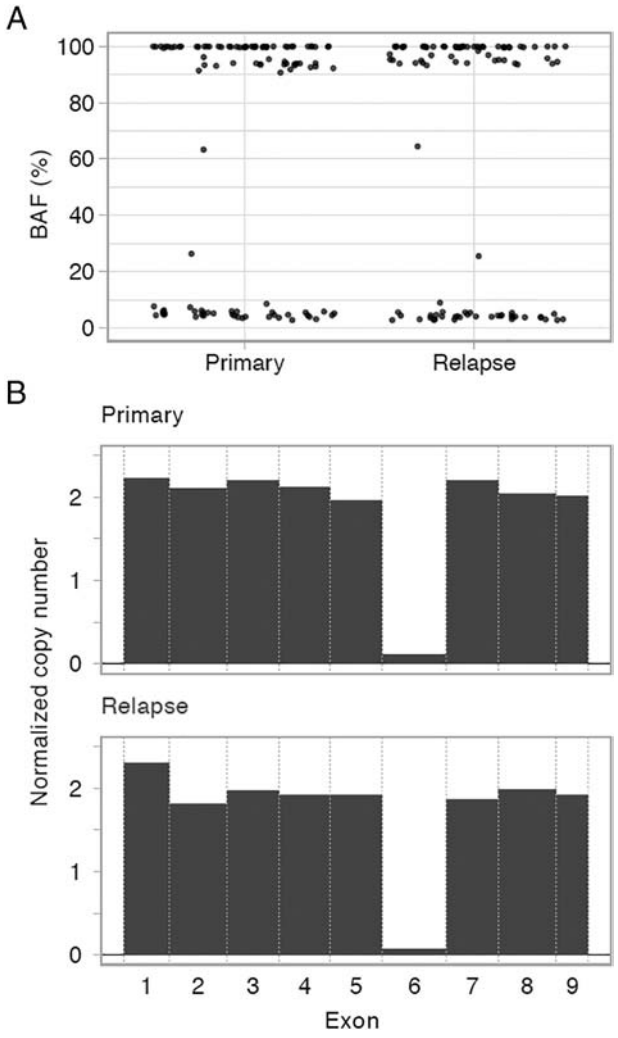

Figure 2. *SMARCB1* deletion in Patient 3. Only exon 6 out of 9 exons of *SMARCB1* was deleted in patient 3, who was diagnosed as having a malignant rhabdoid tumor. There was loss of heterozygosity in chromosome 22 in this patient, resulting in homozygous deletion of *SMARCB1* exon 6.

remission with salvage treatment after relapse or progression. Except for one patient diagnosed with ganglioneuroblastoma, none of the patients in group 3 responded to primary and secondary therapy. The overall survival rate tended to be higher in group 1 than in group 3, although the difference was not significant (P = .125). Progression-free survival was significantly better in group 1 and worse in group 3 (P = .011) (Figure 4). Interestingly, the two patients (patients 4 and 9) whose recurrent samples only had concordant mutations, with no newly acquired SNVs/InDels, showed late relapse more than 2 years after initial diagnosis.

The number of newly acquired SNVs/InDels in the three patients who had received radiotherapy to the biopsy sites at relapse (patients 6, 7, 16) was significantly higher than that of the other patients (5.33 ± 2.31 vs 1.38 ± 1.59, P = .017).

Low-VAF Variants and Low-Level CNAs

Among the SNVs/InDels detected in only recurrent lesions, 71% of variants had low VAF values of less than 10% (Figure 5). However, only 5% of SNVs/InDels detected in both lesions had low VAF values. The low-VAF variants include possible disrupting mutations of tumor suppressor genes *RB1*, *TP53*, *BCOR*, *APC*, *TSC2*, *BRCA2*, and *TGFBR2*, and possible driver mutations of oncogenes *EGFR* and *HRAS*. These mutations might have important roles in tumorigenesis and tumor progression. Moreover, several clinically actionable variants such as *CDK6*, *PTCH1*, *SMO*, and *EGFR* were detected with low VAF values in the recurrent lesions.

We detected 488 low-level copy number gains and 623 low-level copy number losses (Supplementary Table S5). Genes with frequent one copy loss were *STAT3* (n = 8), *PBRM1* (n = 7), *GNA11* (n = 7), *FGF3* (n = 6),

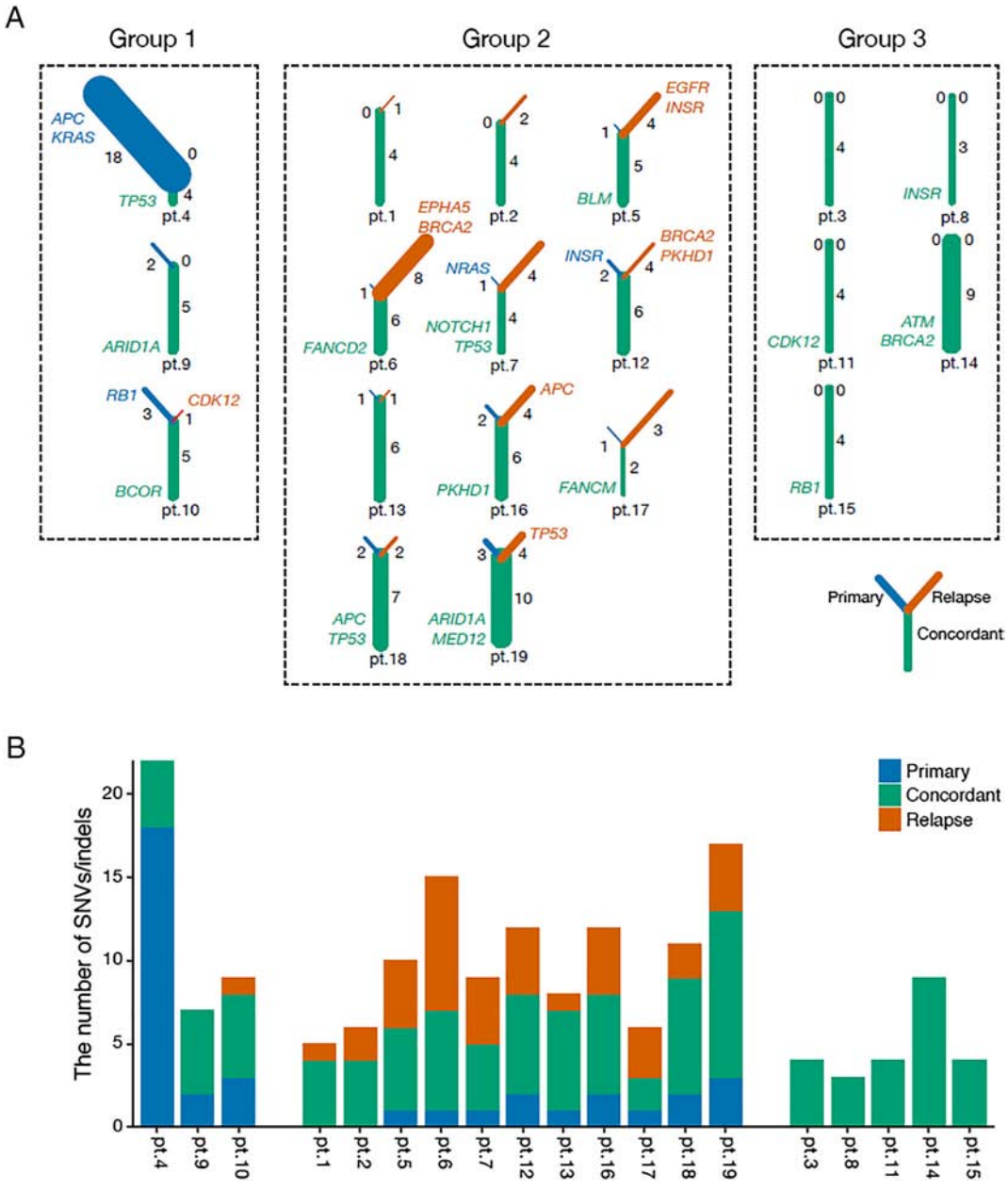

Figure 3. Groups according to the mutational change pattern. Patients were divided into three groups. A subject was classified into group 1 when the number of disappeared SNVs and InDels in the recurrent lesion was more than the number of newly occurring SNVs and InDels. A subject was classified into group 2 when the number of disappeared SNVs and InDels was less than or equal to the number of newly occurring SNVs and InDels. A subject was classified into group 3 when no SNVs or InDels disappeared or newly occurred.

Table 3. Comparison of Treatment Responses among the Three Groups

	Group 1 (*N* = 3)	Group 2 (*N* = 11)	Group 3 (*N* = 5)	*P*
Age, median (range), yr	14.4 (12.8-15.3)	8.8 (2.7-18.5)	3.0 (0.3-13.8)	.071
Sex				1
- Female	1 (33.3%)	6 (54.5%)	2 (40.0%)	
- Male	2 (66.7%)	5 (45.5%)	3 (60.0%)	
Radiotherapy				.716
- Not done	3 (100.0%)	8 (72.7%)	5 (100.0%)	
- Done	0 (0.0%)	3 (27.3%)	0 (0.0%)	
Timing of progression				.184
- Progression during treatment	1 (33.3%)	3 (27.3%)	4 (80.0%)	
- Relapse after treatment	2 (66.7%)	8 (72.7%)	1 (20.0%)	
Response to second-line treatment				.105
- CR	3 (100.0%)	2 (18.2%)	1 (20.0%)	
- PR	0 (0.0%)	2 (18.2%)	0 (0.0%)	
- Progression	0 (0.0%)	7 (63.6%)	4 (80.0%)	
Progression-free survival (median), months	25.31	15.64	6.07	.011 *
Overall survival (median), months	NA	25.1	22.3	.125

Abbreviations: *CR*, complete remission; *PR*, partial remission.
* Significant difference.

ATM (*n* = 6), *PGR* (*n* = 6), *CRKL* (*n* = 6), *TP53* (*n* = 6), and *HSP90AA1* (*n* = 6). Among them, the copy number loss of tumor suppressor genes *PBRM1*, *ATM*, and *TP53* might have important roles. *PGR* is located 7 Mbp apart from *ATM*, and all copy number losses co-presented with *ATM* copy number losses.

Discussion

In this study, we characterized genomic alterations between diagnostic and recurrent lesions in patients with relapsed/refractory pediatric solid tumors by performing targeted deep sequencing using a custom-designed cancer panel. This platform enabled the sensitive detection of genomic alterations in both diagnostic and recurrent lesions, including the identification of variants with low VAF values. Patients were divided into three groups according to the pattern of SNVs/InDels between the diagnostic and recurrent lesions, and there was an association between the pattern and the clinical outcome.

It is not easy to obtain tissue again when the tumor recurs in pediatric patients; therefore, there have been few studies comparing the genomics between diagnostic and relapsed samples in pediatric cancer. Previous studies were limited to leukemia, neuroblastoma, and medulloblastoma, and these studies utilized whole exome sequencing or whole genome sequencing, with or without whole transcriptome analysis [29–32]. These studies demonstrated the clonal evolution of cancer from diagnosis to relapse, irrespective of the diagnosis or the analytic method. The differences in our study were that our study examined various pediatric solid tumors and used targeted deep sequencing.

Targeted deep sequencing has many advantages, including the relative simplicity of the method to detect known variants, with high coverage and low complexity [33]. The presence of many variants with a VAF under 10% in the recurrent lesions made it clear that very high-depth panel sequencing offers advantages in a clinical setting. Although assessing whether these low VAF mutations have a role as driver rather than passenger mutations is difficult, low-VAF variants could be as important as high-VAF variants in clinical specimens [10]. These variants could be informative because they may be associated with tumor heterogeneity or subclonal changes after cancer treatment [34]. In our study, several oncogenic variants, including those in *TP53, APC, BRCA2*, and *EGFR*, and actionable variants such as *EGFR*, *CDK6*, *PTCH1*, and *SMO* were detected with low VAF values in the recurrent lesions. Standard sequencing (typically 100-200× obtained by exome-only coverage, or 30-60× obtained by full genome coverage) would not have sufficient sensitivity to detect these exonic variants [11,13].

When we classified our patients into three categories based on the pattern of mutations after cancer treatment, we found a significant association between clinical outcome and the major patterns of these alterations. Especially, patients in group 1, whose recurrent samples indicated clonal extinction in response to cancer treatment showed longer progression-free survival compared with patients in group 2, whose recurrent samples indicated additional localized clonal expansion after cancer treatment. Furthermore, all patients in group 1 achieved complete remission after relapse. Based on these results, we speculated that subclonal changes under the selective pressure of cancer therapy might be associated with clinical outcome, and clonal expansion during cancer therapy has a role in treatment resistance in childhood cancer [7,34–36]. Interestingly, except for one patient, patients in group 3, whose genetic profile only had concordant mutations with no newly acquired or disappearing SNVs/InDels, showed the worst clinical outcomes and did not respond to primary and secondary therapy. These findings suggest that a lack of subclonal changes in response to cancer therapy revealed a poor outcome and

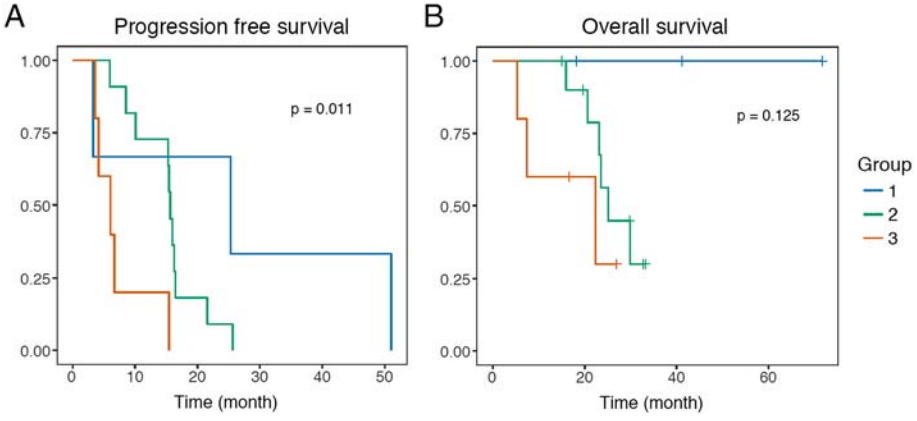

Figure 4. Survival graph according to the group. (A) Progression-free survival was significantly better in group 1 and worse in group 3 (*P* = .011). (B) The overall survival rate tended to be higher in group 1 than in group 3, although it was not significant (*P* = .125).

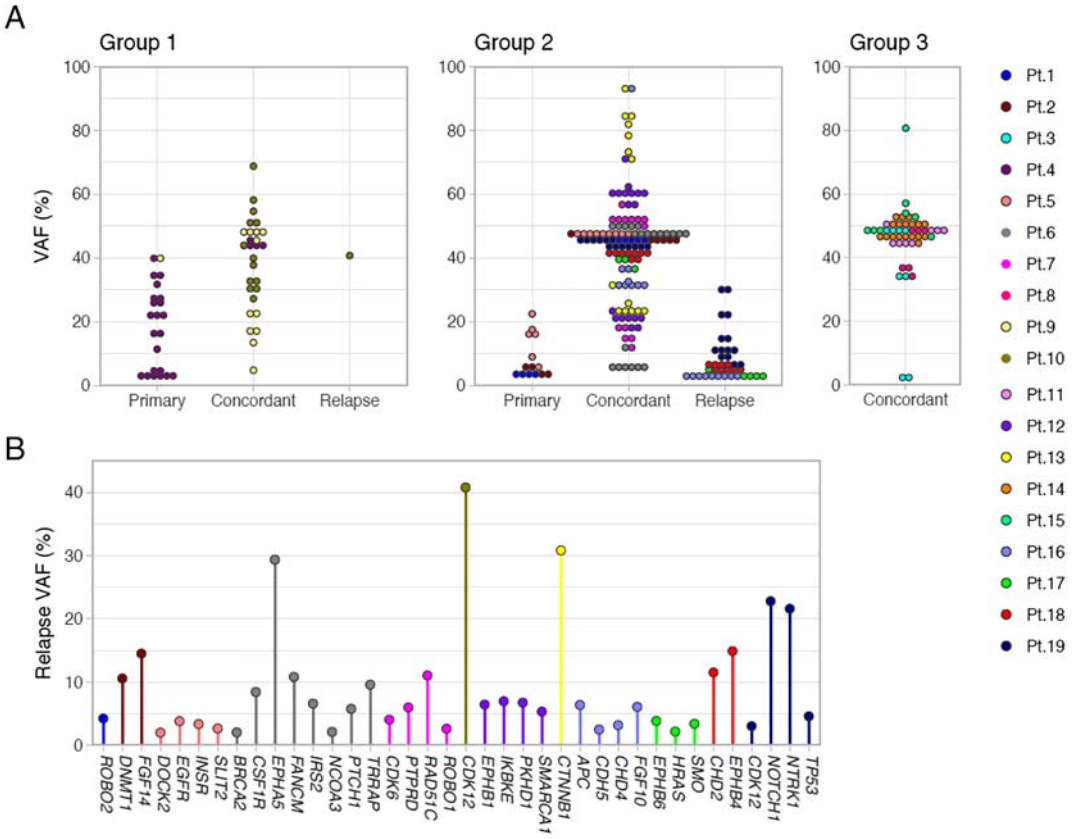

Figure 5. VAFs of SNVs and InDels. (A) VAFs of SNV and InDels are shown. (B) Variants occurring only in recurrent lesions are shown. Among SNVs and InDels detected only in recurrent lesions, 71% of variants have low VAFs of less than 10%, and these variants included many possible pathogenic or actionable variants.

has a prognostic value. However, it is unclear whether resistance is predominantly driven by preexisting concordant mutations or *de novo* alterations outside of the target panel. Other potential causes such as transcriptomic and epigenetic factors should be considered.

In our cohort, the tumor mutation burden was significantly increased in recurring tumors of patients who received radiotherapy at the biopsy site. Ionizing radiation is a well-known mutagen and has been considered a factor in the development of secondary neoplasm [37,38]. By contrast, tumor mutation burden is an important predictor of response to immune checkpoint inhibitors in adult cancers [39,40]. Although immunotherapy for pediatric solid tumors is under investigation [41], a combination of immunotherapy and radiotherapy may have potential to improve the effect of immunotherapy [42].

Conclusion

In this study, we characterized genomic changes in recurrent childhood cancers. A number of variants in the relapsed samples had low VAFs, suggesting the usefulness of targeted deep sequencing to detect oncogenic or actionable variants in the relapsed samples. In addition, the detected mutational change patterns were related to the clinical outcome of the patients. These findings could help to understand the biology of relapsed childhood cancer and to develop personalized treatment strategies based on the genetic profile of childhood cancers.

Supplementary data to this article can be found online at https://doi.org/10.1016/j.tranon.2018.08.013.

Acknowledgements

The biospecimens for this study were provided by Samsung Medical Center BioBank.

Funding sources

This study was supported by a grant from the National R&D Program for Cancer Control, Ministry of Health and Welfare, Republic of Korea (No. 1520210) and the Korea Health Technology R&D Project through the Korea Health Industry Development Institute (KHIDI), Ministry of Health & Welfare, Republic of Korea (HI14C3418).

References

[1] Gatta G, Botta L, Rossi S, Aareleid T, Bielska-Lasota M, Clavel J, Dimitrova N, Jakab Z, Kaatsch P, and Lacour B, et al (2014). Childhood cancer survival in Europe 1999-2007: results of EUROCARE-5—a population-based study. *Lancet Oncol* **15**, 35–47.

[2] Lawrence MS, Stojanov P, Polak P, Kryukov GV, Cibulskis K, Sivachenko A, Carter SL, Stewart C, Mermel CH, and Roberts SA, et al (2013). Mutational heterogeneity in cancer and the search for new cancer-associated genes. *Nature* **499**, 214–218.

[3] Worst BC, van Tilburg CM, Balasubramanian GP, Fiesel P, Witt R, Freitag A, Boudalil M, Previti C, Wolf S, and Schmidt S, et al (2016). Next-generation personalised medicine for high-risk paediatric cancer patients—the INFORM pilot study. *Eur J Cancer* **65**, 91–101.

[4] Ding L, Ley TJ, Larson DE, Miller CA, Koboldt DC, Welch JS, Ritchey JK, Young MA, Lamprecht T, and McLellan MD, et al (2012). Clonal evolution in relapsed acute myeloid leukaemia revealed by whole-genome sequencing. *Nature* **481**, 506–510.

[5] Juskevicius D, Dirnhofer S, and Tzankov A (2017). Genetic background and evolution of relapses in aggressive B-cell lymphomas. *Haematologica* **102**, 1139–1149.
[6] Wu C, de Miranda NF, Chen L, Wasik AM, Mansouri L, Jurczak W, Galazka K, Dlugosz-Danecka M, Machaczka M, and Zhang H, et al (2016). Genetic heterogeneity in primary and relapsed mantle cell lymphomas: impact of recurrent CARD11 mutations. *Oncotarget* **7**, 38180–38190.
[7] Asic K (2016). Dominant mechanisms of primary resistance differ from dominant mechanisms of secondary resistance to targeted therapies. *Crit Rev Oncol Hematol* **97**, 178–196.
[8] Chen K, Meric-Bernstam F, Zhao H, Zhang Q, Ezzeddine N, Tang LY, Qi Y, Mao Y, Chen T, and Chong Z, et al (2015). Clinical actionability enhanced through deep targeted sequencing of solid tumors. *Clin Chem* **61**, 544–553.
[9] Frampton GM, Fichtenholtz A, Otto GA, Wang K, Downing SR, He J, Schnall-Levin M, White J, Sanford EM, and An P, et al (2013). Development and validation of a clinical cancer genomic profiling test based on massively parallel DNA sequencing. *Nat Biotechnol* **31**, 1023–1031.
[10] Shin HT, Choi YL, Yun JW, Kim NKD, Kim SY, Jeon HJ, Nam JY, Lee C, Ryu D, and Kim SC, et al (2017). Prevalence and detection of low-allele-fraction variants in clinical cancer samples. *Nat Commun* **8**1377.
[11] Lee C, Bae JS, Ryu GH, Kim NKD, Park D, Chung J, Kyung S, Joung JG, Shin HT, and Shin SH, et al (2017). A method to evaluate the quality of clinical gene-panel sequencing data for single-nucleotide variant detection. *J Mol Diagn* **19**, 651–658.
[12] Li H and Durbin R (2009). Fast and accurate short read alignment with Burrows-Wheeler transform. *Bioinformatics* **25**, 1754–1760.
[13] Cibulskis K, Lawrence MS, Carter SL, Sivachenko A, Jaffe D, Sougnez C, Gabriel S, Meyerson M, Lander ES, and Getz G (2013). Sensitive detection of somatic point mutations in impure and heterogeneous cancer samples. *Nat Biotechnol* **31**, 213–219.
[14] Wilm A, Aw PP, Bertrand D, Yeo GH, Ong SH, Wong CH, Khor CC, Petric R, Hibberd ML, and Nagarajan N (2012). LoFreq: a sequence-quality aware, ultra-sensitive variant caller for uncovering cell-population heterogeneity from high-throughput sequencing datasets. *Nucleic Acids Res* **40**, 11189–11201.
[15] Ye K, Schulz MH, Long Q, Apweiler R, and Ning Z (2009). Pindel: a pattern growth approach to detect break points of large deletions and medium sized insertions from paired-end short reads. *Bioinformatics* **25**, 2865–2871.
[16] Pugh TJ, Morozova O, Attiyeh EF, Asgharzadeh S, Wei JS, Auclair D, Carter SL, Cibulskis K, Hanna M, and Kiezun A, et al (2013). The genetic landscape of high-risk neuroblastoma. *Nat Genet* **45**, 279–284.
[17] Shern JF, Chen L, Chmielecki J, Wei JS, Patidar R, Rosenberg M, Ambrogio L, Auclair D, Wang J, and Song YK, et al (2014). Comprehensive genomic analysis of rhabdomyosarcoma reveals a landscape of alterations affecting a common genetic axis in fusion-positive and fusion-negative tumors. *Cancer Discov* **4**, 216–231.
[18] Wu X, Dagar V, Algar E, Muscat A, Bandopadhayay P, Ashley D, and Wo Chow C (2008). Rhabdoid tumour: a malignancy of early childhood with variable primary site, histology and clinical behaviour. *Pathology* **40**, 664–670.
[19] Sullivan LM, Folpe AL, Pawel BR, Judkins AR, and Biegel JA (2013). Epithelioid sarcoma is associated with a high percentage of SMARCB1 deletions. *Mod Pathol* **26**, 385–392.
[20] Kim J, Lee K, and Pelletier J (1998). The desmoplastic small round cell tumor t (11;22) translocation produces EWS/WT1 isoforms with differing oncogenic properties. *Oncogene* **16**, 1973–1979.
[21] Morrow JJ and Khanna C (2015). Osteosarcoma genetics and epigenetics: emerging biology and candidate therapies. *Crit Rev Oncog* **20**, 173–197.
[22] Choy E, Hornicek F, MacConaill L, Harmon D, Tariq Z, Garraway L, and Duan Z (2012). High-throughput genotyping in osteosarcoma identifies multiple mutations in phosphoinositide-3-kinase and other oncogenes. *Cancer* **118**, 2905–2914.
[23] Behjati S, Tarpey PS, Sheldon H, Martincorena I, Van Loo P, Gundem G, Wedge DC, Ramakrishna M, Cooke SL, and Pillay N, et al (2014). Recurrent PTPRB and PLCG1 mutations in angiosarcoma. *Nat Genet* **46**, 376–379.
[24] Murali R, Chandramohan R, Moller I, Scholz SL, Berger M, Huberman K, Viale A, Pirun M, Socci ND, and Bouvier N, et al (2015). Targeted massively parallel sequencing of angiosarcomas reveals frequent activation of the mitogen activated protein kinase pathway. *Oncotarget* **6**, 36041–36052.
[25] Ruteshouser EC, Robinson SM, and Huff V (2008). Wilms tumor genetics: mutations in WT1, WTX, and CTNNB1 account for only about one-third of tumors. *Genes Chromosomes Cancer* **47**, 461–470.
[26] Eichenmuller M, Trippel F, Kreuder M, Beck A, Schwarzmayr T, Haberle B, Cairo S, Leuschner I, von Schweinitz D, and Strom TM, et al (2014). The genomic landscape of hepatoblastoma and their progenies with HCC-like features. *J Hepatol* **61**, 1312–1320.
[27] Jones C, Karajannis MA, Jones DTW, Kieran MW, Monje M, Baker SJ, Becher OJ, Cho YJ, Gupta N, and Hawkins C, et al (2017). Pediatric high-grade glioma: biologically and clinically in need of new thinking. *Neuro Oncol* **19**, 153–161.
[28] Pugh TJ, Weeraratne SD, Archer TC, Krummel DAP, Auclair D, Bochicchio J, Carneiro MO, Carter SL, Cibulskis K, and Erlich RL, et al (2012). Medulloblastoma exome sequencing uncovers subtype-specific somatic mutations. *Nature* **488**, 106–110.
[29] Morrissy AS, Garzia L, Shih DJ, Zuyderduyn S, Huang X, Skowron P, Remke M, Cavalli FM, Ramaswamy V, and Lindsay PE, et al (2016). Divergent clonal selection dominates medulloblastoma at recurrence. *Nature* **529**, 351–357.
[30] Schramm A, Koster J, Assenov Y, Althoff K, Peifer M, Mahlow E, Odersky A, Beisser D, Ernst C, and Henssen AG, et al (2015). Mutational dynamics between primary and relapse neuroblastomas. *Nat Genet* **47**, 872–877.
[31] Eleveld TF, Oldridge DA, Bernard V, Koster J, Daage LC, Diskin SJ, Schild L, Bentahar NB, Bellini A, and Chicard M, et al (2015). Relapsed neuroblastomas show frequent RAS-MAPK pathway mutations. *Nat Genet* **47**, 864–871.
[32] Farrar JE, Schuback HL, Ries RE, Wai D, Hampton OA, Trevino LR, Alonzo TA, Guidry Auvil JM, Davidsen TM, and Gesuwan P, et al (2016). Genomic profiling of pediatric acute myeloid leukemia reveals a changing mutational landscape from disease diagnosis to relapse. *Cancer Res* **76**, 2197–2205.
[33] Newman WG and Black GC (2014). Delivery of a clinical genomics service. *Genes (Basel)* **5**, 1001–1017.
[34] Bhang HEC, Ruddy DA, Radhakrishna VK, Caushi JX, Zhao R, Hims MM, Singh AP, Kao I, Rakiec D, and Shaw P, et al (2015). Studying clonal dynamics in response to cancer therapy using high-complexity barcoding. *Nat Med* **21**, 440–448.
[35] Hata AN, Niederst MJ, Archibald HL, Gomez-Caraballo M, Siddiqui FM, Mulvey HE, Maruvka YE, Ji F, Bhang HEC, and Radhakrishna VK, et al (2016). Tumor cells can follow distinct evolutionary paths to become resistant to epidermal growth factor receptor inhibition. *Nat Med* **22**, 262–269.
[36] Misale S, Di Nicolantonio F, Sartore-Bianchi A, Siena S, and Bardelli A (2014). Resistance to anti-EGFR therapy in colorectal cancer: from heterogeneity to convergent evolution. *Cancer Discov* **4**, 1269–1280.
[37] Sherborne AL, Davidson PR, Yu K, Nakamura AO, Rashid M, and Nakamura JL (2015). Mutational analysis of ionizing radiation induced neoplasms. *Cell Rep* **12**, 1915–1926.
[38] Bhatia S and Sklar C (2002). Second cancers in survivors of childhood cancer. *Nat Rev Cancer* **2**, 124–132.
[39] Rizvi NA, Hellmann MD, Snyder A, Kvistborg P, Makarov V, Havel JJ, Lee W, Yuan JD, Wong P, and Ho TS, et al (2015). Mutational landscape determines sensitivity to PD-1 blockade in non-small cell lung cancer. *Science* **348**, 124–128.
[40] Snyder A, Makarov V, Merghoub T, Yuan J, Zaretsky JM, Desrichard A, Walsh LA, Postow MA, Wong P, and Ho TS, et al (2014). Genetic basis for clinical response to CTLA-4 blockade in melanoma. *N Engl J Med* **371**, 2189–2199.
[41] Huang MA, Krishnadas DK, and Lucas KG (2015). Cellular and antibody based approaches for pediatric cancer immunotherapy. *J Immunol Res* 675269.
[42] Twyman-Saint Victor C, Rech AJ, Maity A, Rengan R, Pauken KE, Stelekati E, Benci JL, Xu BH, Dada H, and Odorizzi PM, et al (2015). Radiation and dual checkpoint blockade activate non-redundant immune mechanisms in cancer. *Nature* **520**, 373–377.